Dynamic Adhesion of T Lymphocytes to Endothelial Cells Revealed by Atomic Force Microscopy

XIAOHUI ZHANG,[1,2] EWA P. WOJCIKIEWICZ, AND VINCENT T. MOY[1]

Department of Physiology and Biophysics, University of Miami School of Medicine, Miami, Florida 33136

The recruitment of T lymphocytes to lymphoid organs or sites of inflammation is a crucial step in adaptive immunity. These processes require endothelial activation and expression of adhesion molecules, including E- and P-selectins, intercellular adhesion molecule-1 (ICAM-1), and vascular cell adhesion molecule-1 (VCAM-1). However, the complete characterization of the adhesion strength and dynamics between lymphocytes and endothelial cells has been hampered by the lack of sensitive quantitative techniques. Here we report on the application of atomic force microscopy to characterize the interaction between individual pairs of living T lymphocytes (i.e., Jurkat cells) and human umbilical vein endothelial cells (HUVECs). The detachment of individual cell–cell conjugates was a complex process involving several step-like rupture events and the viscoelastic deformation of cells on the scale of several microns. Adhesion between Jurkat cells and activated endothelial cells increased with compression force and contact time, with the most dramatic changes occurring within the first half second of contact. After 0.25 sec of contact, E-selectin, ICAM-1, and VCAM-1 contributed to 18%, 39%, and 41% of total adhesion strength, respectively, suggesting that ICAM-1 and VCAM-1 contributed more than the selectins in supporting cell attachment. Exp Biol Med 231:1306–1312, 2006

Key words: T lymphocyte; vascular endothelial cell; atomic force microscopy; cell adhesion

Introduction

T lymphocytes are one of the key players in the adaptive immune system. They serve a variety of functions including the identification of specific foreign antigens in the body, and the activation and deactivation of other immune cells (1). Recruitment of lymphocytes from peripheral blood into sites of inflammation or infection supports both the clearance of viral pathogens and the development of many immune system disorders, including asthma, lupus, and rheumatoid arthritis. The first step in this recruitment is the arrest of circulating lymphocytes in microvasculature of the inflamed tissue (2). This process is initiated by the interaction between lymphocytes and vascular endothelial cells via engagement of different sets of cell adhesion molecules (3, 4). When tissues are exposed to an inflammatory stimulus such as cytokines, local endothelial cells will upregulate their expression of P- and E-selectins and integrin ligands, including intercellular adhesion molecule-1 (ICAM-1), and vascular cell adhesion molecule-1 (VCAM-1) (5). Circulating lymphocytes entering the inflamed tissue are captured by the endothelium via interactions mediated by L-selectin expressed on lymphocytes, or by P- and E-selectins expressed on endothelial cells. Subsequent rolling of the captured lymphocytes along the endothelial layer enables lymphocytes to survey the endothelial surface for chemotactic signals. When appropriate signals are encountered, lymphocyte surface integrins are activated and bind tightly to their endothelial ligands. These interactions allow the lymphocyte to slow down and transmigrate across the endothelial layer (6, 7).

T-cell–endothelial interactions have been widely studied. A number of experimental approaches have been employed to characterize the events leading up to extravasation. Early applications include static adhesion assays, parallel plate flow chambers, and Boyden chemotaxis assay (8). Recent advancement in two-photon intravital microscopy further revealed in greater detail the interaction between T cells and the endothelium *in vivo* (8–10). However, there are only limited studies carried out that provide quantitative measurements of the forces that support

These studies were supported in part by grants from the AHA, NSF-BITC and the NIH (GM55611) to VTM, and a fellowship grant (0215139B) from the AHA to XZ.

[1] To whom correspondence should be addressed at Dr. Xiaohui Zhang, The CBR Institute for Biomedical Research, Harvard Medical School, Boston, MA 02115. E-mail: xzhang@cbr.med.harvard.edu; or Dr. Vincent T. Moy, Department of Physiology and Biophysics, University of Miami School of Medicine, 1600 NW 10th Avenue, Miami, Florida 33136. E-mail: vmoy@miami.edu

[2] Current address: The CBR Institute for Biomedical Research, Harvard Medical School, Boston, MA 02115.

Received December 1, 2005.
Accepted March 13, 2006.

1535-3702/06/2318-1306$15.00

the interactions between these two cell types. In this work, we have adapted the atomic force microscope (AFM) (11, 12) to assess the adhesion dynamics of the T-cell–endothelial interaction.

Materials and Methods

Cell Culture. The human T-leukemic cell line Jurkat E6–1 was obtained from ATCC (Manassas, VA) and maintained in RPMI 1640 medium (Gibco BRL, Carlsbad, CA) supplemented with 10% fetal bovine serum (FBS), 1% glutamine, 50 U/ml penicillin, and 50 μg/ml streptomycin in 5% CO_2 at 37°C. Human umbilical vein endothelial cells (HUVECs) were purchased from Cambrex (Walkersville, MD) and cultured in endothelial cell basal medium (EBM-2) supplemented with 2% FBS, hydrocortisone, human fibroblast growth factor (hFGF), vascular endothelial growth factor (VEGF), insulin-like growth factor-1 (IGF-1), ascorbic acid, human epidermal growth factor (hEGF), Gentamicin-Amphotericin, and heparin. HUVECs were plated on 35-mm tissue culture dishes (Becton Dickinson, Franklin Lakes, NJ) and were used between passages 5 and 7. To mimic an activated endothelium, HUVECs were stimulated by the proinflammatory cytokine tumor necrosis factor-α (TNF-α) for 6 hrs prior to force measurements.

Proteins and Other Reagents. Human TNF-α and function-blocking antibodies BBIG-E4 (anti–E-selectin), BBIG-I1 (anti–ICAM-1), and AF809 (anti–VCAM-1) were purchased from R&D Systems (Minneapolis, MN). In function-blocking experiments HUVECs were incubated with inhibitory antibodies (50 μg/ml each) for 30 min prior to the force measurements. All other reagents were purchased from Sigma (St. Louis, MO).

T-cell Adhesion Measured by Atomic Force Microscopy. The experimental apparatus used to measure cell adhesion is schematically illustrated in Figure 1A (13). HUVECs were plated on standard 35-mm tissue culture dishes while a single Jurkat cell was coupled to the end of the AFM cantilever (Fig. 1B). Atomic force microscopy was used to control the relative position of the interacting cells via expansion or contraction of the piezoelectric translator (P-841; Physik Instrumente, Waldbronn, Germany). The force acting between the cells was derived from the deflection of the AFM cantilever, which was monitored by reflecting a focused laser beam off the back of the cantilever into a 2-segment photodiode. Cantilevers (MLCT-AUHW; Veeco Probes, Santa Barbara, CA) were individually calibrated by thermal fluctuation analysis according to the method of Hutter and Bechhoefer (14) and had spring constants of approximately 0.010 N/m.

The AFM force measurements were carried out with individual Jurkat cells attached to the tip of an AFM cantilever via a Concanavalin A (Con A)–mediated linkages (15–17). The cantilevers were first incubated in 0.5 mg/ml biotinamidocaproyl-labeled bovine serum albumin (BSA) overnight at 37°C, then rinsed with phosphate-buffered

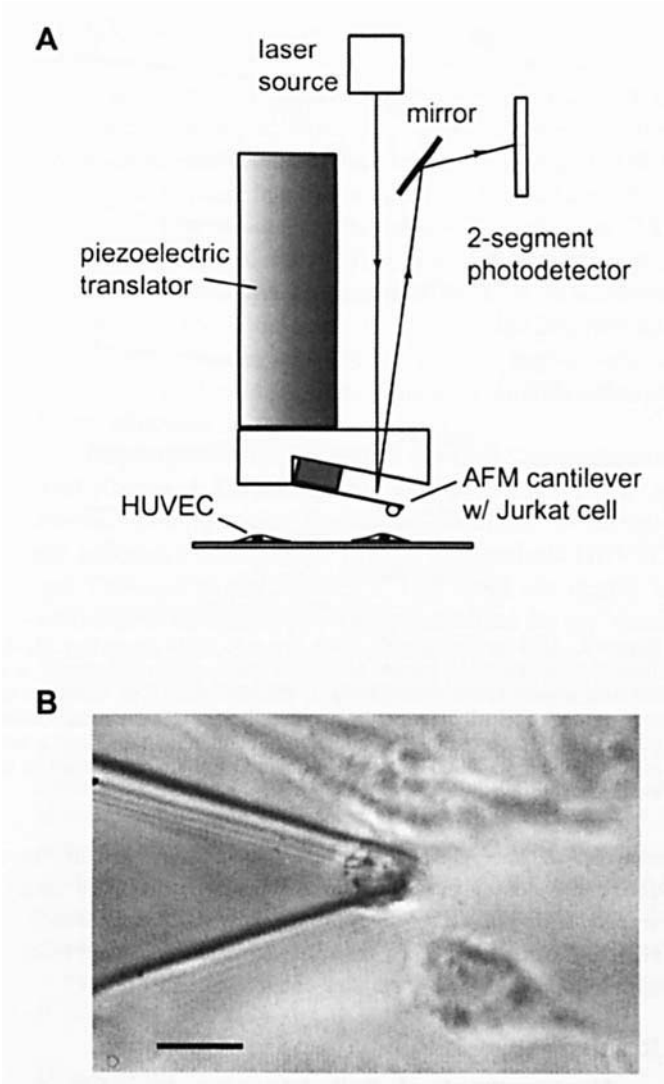

Figure 1. (A) Schematics of the AFM design used in this study. (B) Micrograph of a Jurkat cell attached to the tip of an AFM cantilever over HUVECs in a tissue culture dish. The bar is 20 μm.

saline (PBS) and incubated in 0.5 mg/ml streptavidin for 10 min at room temperature. Next, the cantilevers were incubated in 0.5 mg/ml biotinylated Con A. With the aid of an optical magnification system situated below the AFM, the tip of the Con A–functionalized cantilever was positioned above the center of a cell and gently lowered onto the cell for approximately 1 sec to attach the cell to the cantilever (Fig. 1B). To obtain an estimate of the strength of the cell–cantilever linkage, we allowed the attached cell to interact with a tissue culture dish coated with Con A for 1 min. Upon retraction of the cantilever, separation always ($N > 20$) occurred between the cell and the Con A–coated surface. The average force needed to induce separation was >2 nN, which was at least twice as large as the detachment forces recorded in this study (<1 nN).

Measurements of lymphocyte–endothelial cell interaction were conducted at 25°C in phenol red–free RPMI 1640 medium (Gibco BRL, Carlsbad, CA) containing 10 m*M* Hepes. At the onset of the measurements the Jurkat cell,

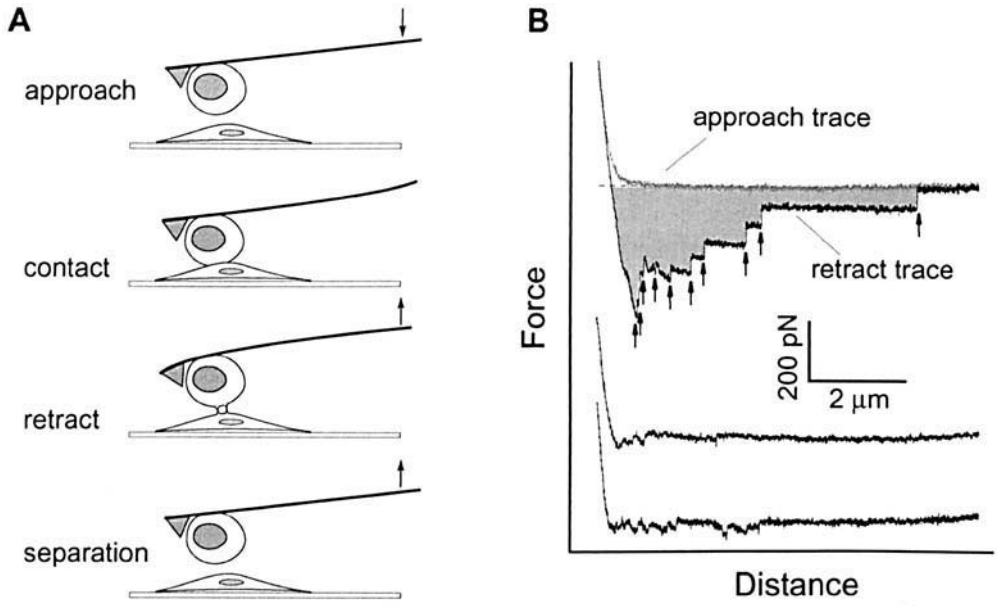

Figure 2. AFM measurements of the Jurkat/HUVEC interaction. (A) Schematic representation of a typical cycle of the AFM measurement. (B) Typical force spectrum traces: strong adhesion occurred between a Jurkat cell and a TNF-α–stimulated HUVEC (top trace). The Jurkat cell adhered weakly to the resting HUVEC (middle trace). The adhesion between the Jurkat cell and the TNF-α–stimulated HUVEC was markedly reduced by a cocktail of blocking antibodies against E-selelectin, ICAM-1, and VCAM-1 (bottom trace). The measurements were acquired with a compression force of 500 pN, 0.25 sec of contact duration, and a cantilever retraction speed of 3 μm/sec. The shaded area in the top trace indicates the work of de-adhesion. Arrows in the top trace point to rupture events such as breakage of adhesive bond(s). The dashed line indicates zero force.

coupled to the AFM cantilever, was positioned directly above the center of an isolated HUVEC in a Petri dish seeded with HUVECs to approximately 20% confluency. Hence, the acquired AFM measurements were derived from interaction between the centers of the two cell bodies.

Results

Measurement of Cell Adhesion by AFM. As illustrated in Figure 2A, AFM measurements of the interaction between an individual Jurkat cell and a HUVEC involves a series of four steps. First, the cantilever with an attached Jurkat cell is lowered onto a HUVEC. At a certain point contact is made, allowing for cell–cell interaction to take place. The cantilever is subsequently retracted via the contraction of the piezoelectric translator, pulling the Jurkat–HUVEC pair apart until complete separation of the 2 cells is achieved. During this process, the AFM continuously monitors the deflection of the cantilever in order to report on the interaction between the Jurkat cell and the HUVEC.

A typical AFM force-displacement record of the interaction between a Jurkat cell and a TNF-α–activated HUVEC is presented in the top trace of Figure 2B. In this figure, the *y* axis plots the cell–cell interaction force as a function of the relative distance between the base of the cantilever and sample (i.e., the HUVEC). At the beginning of the force measurement, when the Jurkat cell is several microns above the HUVEC, there was no strain on the cantilever. At this position, which is marked by a dashed line in the upper trace of Figure 2B, the force was zero. Expansion of the piezoelectric translator lowered the Jurkat cell onto the HUVEC. Following cell–cell contact, further expansion of the translator pressed the Jurkat cell against the HUVEC. The compression force felt by the cells was determined from the upward deflection of the cantilever. For the measurements shown in Figure 2B, the predefined limit of the compression force was set at 500 pN. Once this force value was reached the expansion of the translator ceased. This compression force was held for a predefined cell–cell contact time (0.25 sec) before the translator contracted to initiate cell–cell separation. Upon retraction of the cantilever, molecular linkages established between the cells pulled the cantilever downward, as illustrated in Figure 2A. The cell detachment process typically involved a series of rupture events, as indicated in the top trace of Figure 2B. Each of these rupture events resulted in a rapid jump in force and may correspond to the unbinding of one or more adhesive ligand–receptor bonds. The magnitudes of the force transitions were between 30 and 100 pN, which are consistent with the reported unbinding forces of individual selectin and integrin bonds (18–20). Complete separation between the two cells did not occur until they were stretched by more than 5 μm in many measurements. By contrast, the interaction between a Jurkat cell and an unstimulated HUVEC (Fig. 2B, middle trace) showed significantly fewer bond-rupturing events than the interaction of a Jurkat cell and a TNF-α–activated HUVEC (top trace).

Relative Contributions of Integrins and Selectins to Cell Adhesion. To quantify the adhesive strength of the interacting cells, we measured the work done by the

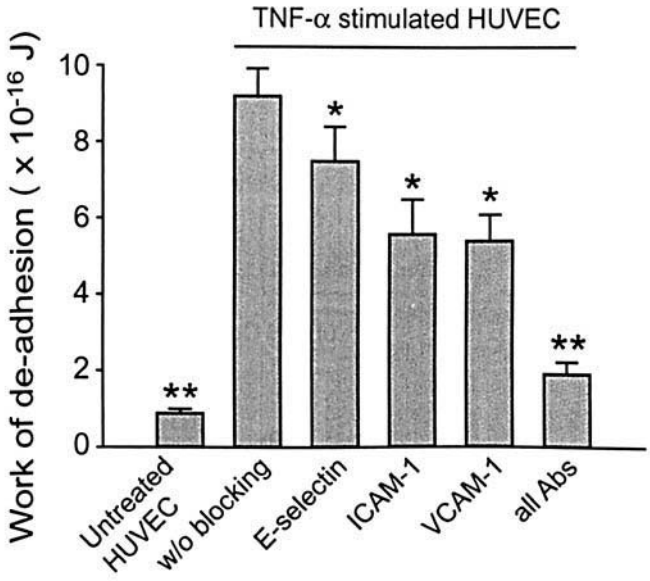

Figure 3. Adhesion strength between a single pair of a Jurkat cell and a HUVEC under different conditions measured by the work of de-adhesion. The measurements were acquired with a compression force of 500 pN, 0.25 sec of contact, and a cantilever retraction speed of 3 μm/s. Neutralizing antibodies used: BBIG-E4 (anti–E-selectin), BBIG-I1 (anti–ICAM-1), and AF809 (anti–VCAM-1). The error bar is standard error with $N > 15$ in each case. $^{*}P < 0.05$ compared with the TNF-α–stimulated HUVEC. $^{**}P < 0.05$ compared with any other groups.

cantilever to separate the cells (16). As indicated by the shaded area in the top trace of Fig. 2B, the work of de-adhesion is derived from integrating the adhesive force over the distance traveled by the cantilever up to the point of the last bond rupture. Unlike the maximal stretching force, which only reflects the force component of the detachment process, the work of de-adhesion accounts for both the work done to break the molecular linkages and the work done to stretch the cells. It is noteworthy to indicate that the work of de-adhesion does not directly reflect the adhesion energy of the cell. It includes all the dissipated energy of the detachment process and the viscoelastic deformation of the cell. Therefore, the work of de-adhesion can be many times larger than the actual adhesion energy of an adherent cell. On average the work of de-adhesion required to separate a Jurkat cell pressed against (500-pN compression force) an activated HUVEC for 250 msec was about 1×10^{-15} J. By contrast, a substantial reduction in the binding of a Jurkat cell to a TNF-α–activated HUVEC was observed following the addition of a cocktail of function-blocking antibodies to E-selectin, VCAM-1, and ICAM-1 (compare Fig. 2B, top and bottom traces) to the level observed for the interaction between a Jurkat cell and an unstimulated HUVEC. Together, these observations demonstrate that the expression of E-selectin, ICAM-1, and VCAM-1 were upregulated in the TNF-α–activated HUVEC and accounted for the majority of the enhanced adhesion to the Jurkat cells.

To more precisely define the relative contributions of the different types of adhesion molecules expressed on the HUVEC surface in supporting lymphocyte adhesion, the inhibition potency of the function-blocking antibodies was examined separately. Figure 3 shows the average work of de-adhesion measured from more than 15 cell–cell pairs. The addition of blocking antibodies to E-selectins, ICAM-1, or VCAM-1 alone induced a partial but significant ($P < 0.05$) inhibition of adhesion between Jurkat cells and TNF-α–activated HUVECs (Fig. 3). While anti–E-selectin antibodies led to an 18% inhibition of work of de-adhesion, both anti–ICAM-1 and anti–VCAM-1 antibodies inhibited Jurkat cell adhesion by 39% and 41%, respectively. A cocktail of all three antibodies resulted in an 80% reduction in cell adhesion.

Dependence of Adhesion on Cell Compression and Contact Duration. As shown in Figure 4A, an increase in compression force from 200 to 800 pN elevated the adhesion of Jurkat cells to both unstimulated HUVECs and TNF-α–activated HUVECs. This trend can largely be attributed to the increase in contact surface as the two elastic cells were pressed against each other. A larger contact surface allowed for greater interaction between the opposing cells. Moreover, adhesion between a Jurkat cell and an activated HUVEC increased after prolonging the duration of contact (Fig. 4B). However, after treatment with three blocking antibodies to E-selectin, ICAM-1, and VCAM-1, adhesion seemed to reach a plateau after 2 secs of contact. Additional prolonging of contact time did not further enhance adhesion. This result strongly suggests that the enhanced adhesion following prolonged cell-to-cell contact is due to the engagement of adhesion molecules E-selectin, ICAM-1, and/or VCAM-1 to their respective receptors.

Discussion

T-lymphocyte adhesion to vascular endothelium is the prerequisite for transendothelial migration, a crucial step in the development of many immune diseases, including rheumatoid arthritis and psoriasis. In this work, we employed the AFM to characterize the interaction of a Jurkat cell and an activated HUVEC as a model system for interaction between a T cell and the endothelium *in vivo*. The Jurkat T-cell line was derived from Epstein Barr virus–negative, non-Hodgkin's lymphoblastic leukemia (21) and has been widely used to study T-cell adhesion, as most native adhesion molecules and related signaling pathways remained functional in this cell line (22, 23). A TNF-α–activated HUVEC is often used as an *in vitro* model of the inflamed endothelium (5, 24). Whereas previous AFM studies employed single molecule measurements to investigate the dynamic strength of a specific cell adhesion molecule (17, 18, 25), the current study examined how different populations of cell adhesion molecules come together to stabilize the T-cell–endothelial interaction. The experimental parameters used in our measurements were intended to mimic conditions encountered during the initial contact between T cells and the endothelium. Assuming a

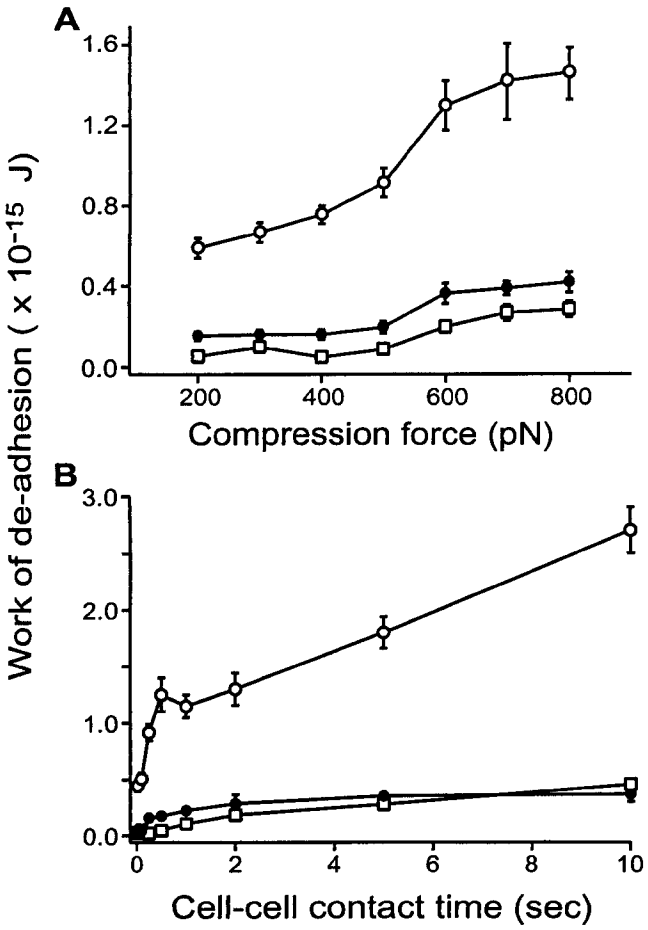

Figure 4. Adhesion strength between a single pair of a Jurkat cell and a HUVEC measured by work of de-adhesion. (A) Effect of compression force for a contact time of 0.25 sec. (B) Effect of contact time for a compression force of 500 pN. Open circles, filled circles, and rectangles represent measurements obtained using TNF-α–activated HUVECs without blocking; with blocking by BBIG-E4 (anti–E-selectin), BBIG-I1 (anti–ICAM-1), and AF809 (anti–VCAM-1) neutralizing antibodies; and unstimulated HUVECs, respectively. The error bar is the standard error with $N > 10$ in each case.

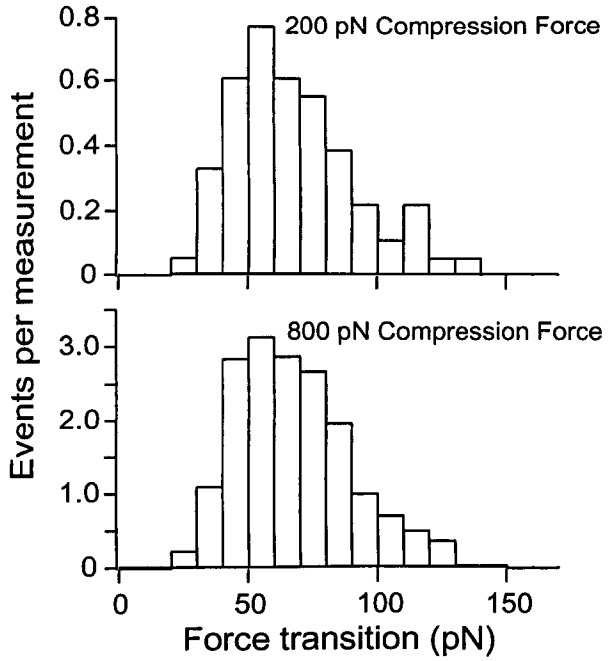

Figure 5. Distribution of rupture forces detected in the detachment of Jurkat/HUVEC conjugates. Top and bottom histograms were acquired from AFM measurements carried out with compression forces of 200 and 800 pN, respectively. Although the number of force jumps is greater at the higher compression force, the normalized histograms are nearly indistinguishable.

Jurkat cell radius of 5 μm and a Young's modulus of 0.5 kPa, we estimate the cell–cell contact areas to be from 5 to 15 μm^2 for the compression forces applied in our study. This estimate of the contact areas is in good agreement with our measurements of the contact area formed by T cells using reflection interference contrast microscopy.[1] Under these conditions, the number of ligand–receptor bonds formed during cell–cell contact was in the range of 3 to 20, as determined from the number of force transitions in the AFM force scan measurements.

Our AFM measurements recorded the tension generated to break the intercellular linkages that hold the interacting cells together as they are being pulled apart by the AFM. From these measurements, we were able to gain some important insight into the dynamics of the cell adhesion process. To begin with, it is clearly evident that the separation of the attached cells does not occur via the simultaneous breakage of the intercellular linkages. In fact, the AFM measurements indicate that there is a sequential breakage of the individual bonds, as the average force transition in the force scans is 70 pN (SD, 20 pN). These force values are within the range of the unitary unbinding force of selectin- and integrin-mediated bonds (18, 19, 26). To assess whether there is greater cooperativity in the unbinding of the intercellular linkages when more linkages were formed, we compared the magnitude and number of force transitions derived from measurements acquired using 200 and 800 pN of compression force (Fig. 5). We found no significant differences in the magnitude of the force transition, suggesting that there is no cooperative unbinding of intercellular linkages. However, the number of force transition increased 3.4-fold, from an average of 5 at 200 pN to 17 at 800 pN of compression force. This increase is consistent with the expected change in the contact surface as a result of the increase in compression force.

Our observation that the intercellular bonds were severed in a sequential fashion implies that the pulling force generated by the AFM may not distribute evenly among the bonds. Figure 6A illustrates one possible model of how a Jurkat cell detaches from a HUVEC. As previously proposed by Bell (27), the pulling force is initially resisted by the bonds at the periphery of the zone of cell–cell contact, whereas the bonds close to the center are unstrained. Increasing the pulling force stretches the cell and applies greater strain on the peripheral bonds, until they

[1] Wojcikiewicz and Moy, unpublished results

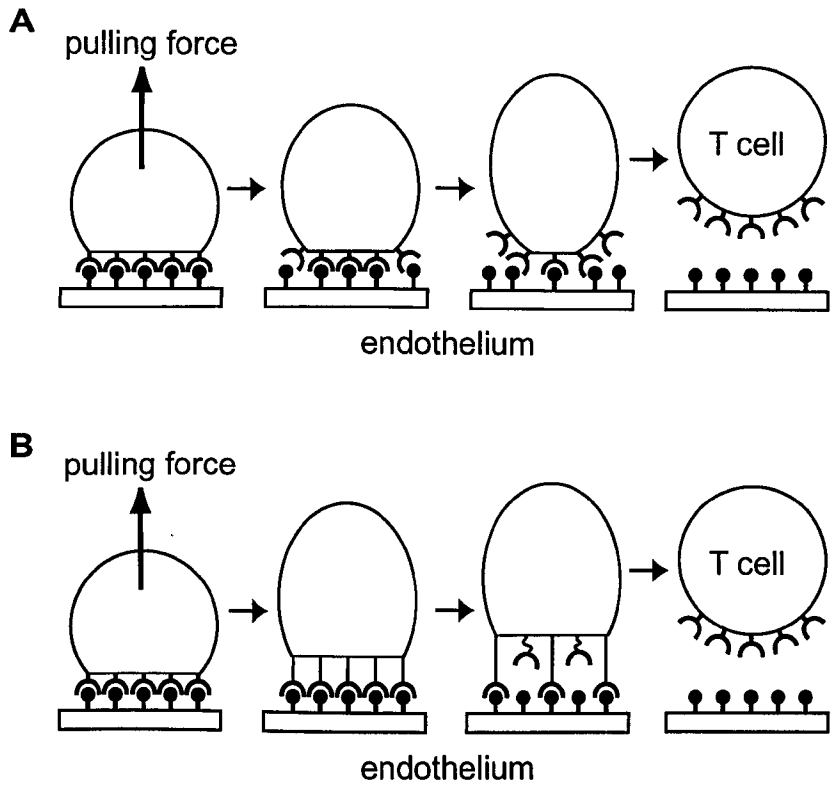

Figure 6. Two possible models of how a T cell detaches from the endothelium. (A) Intercellular adhesion bonds in the periphery of the contact zone are exposed to greater pulling forces than those in the center; therefore, unbinding starts in the periphery and spreads into the center. The process is accompanied by a global viscoelastic deformation of the cell. (B) Pulling results in the formation of intercellular tethers; loads are distributed evenly among all the tethered bonds. Bonds may be severed for any region within the contact zone. Complete cell–cell separation does not occur until all tethered bonds are ruptured.

eventually break. The breakage of these bonds reduces the zone of cell–cell contact, thus permitting greater deformation of the cells. As the cantilever continues to retract, pulling the cells further apart, the process continues until the last bond is severed.

The AFM measurements revealed that the cells undergo gross viscoelastic deformation on the scale of several microns during the cell–cell de-adhesion process. This viscous deformation is frequently observed beyond 3 microns. However, in many cases, long elongations are not necessarily accompanied by an increase in pulling force (Fig. 2B, top trace). Thus, it is conceivable that the observed cell deformation can be attributed to a localized viscoelastic deformation of the cell membrane, such as the formation of membrane tethers (28). Figure 6B illustrates a second possible model of T-cell detachment. In this model, instead of undergoing global cellular deformation, tethers are extruded from cell membranes due to the stretch of cell surface receptors. Since the Jurkat cell membrane is at least one order of magnitude softer than that of the HUVECs,[2] tethers are expected to be extruded mainly from Jurkat cells. These tethers equally sense the force, regardless of whether they are located in the center or at the periphery. As separation continues, intercellular bonds are ruptured in a random manner within the contact zone, until a complete separation is achieved. Future experiments will verify which of the two proposed models more closely resembles our experimental system.

Our measurements also revealed that cell adhesion is dependent on the duration of cell–cell contact. In experiments in which the contact time was varied from 0.02 sec to 10 secs we found that adhesion increased dramatically within the first 0.5 sec of contact before proceeding to a second phase, where adhesion increased more gradually (Fig. 4B). We propose that the first phase stems from the interaction of adhesion molecules within the region of cell–cell contact. The adhesive interaction achieved in this initial phase might be sufficient to establish firm cell adhesion. The second, slower phase, which further stabilizes the cell–cell conjugate, can be attributed to the slow redistribution and lateral movement of adhesion receptors initially outside of the contact area.

We elected to concentrate on measurements acquired with a compression force of 500 pN and a contact time of 250 msec. Under these conditions the number of molecular bonds between the Jurkat cell and the HUVEC is about 10, a sufficient number to arrest the rolling cell (27). Moreover, Figure 4B reveals that a 250-msec contact time was sufficient to complete the initial rapid rise in adhesion.

[2] Zhang and Moy, unpublished results

Under these conditions our force measurements revealed that the endothelial surface adhesion molecules E-selectin, ICAM-1, and VCAM-1 contributed to 18%, 39%, and 41% of total adhesive strength, respectively, between a Jurkat cell and an activated HUVEC, confirming that the Jurkat cells are more dependent on integrins for firm adhesion to the endothelium. However, it is conceivable that this relative contribution of the adhesion molecules is cell type specific and dependent not only on the endothelial adhesion molecules but also on their receptors on lymphocyte surfaces and their activation states. In the Jurkat cell, both LFA-1 (ICAM-1 receptor) and VLA-4 (VCAM-1 receptor) are highly expressed (confirmed by FACS, data not shown), and one would expect these integrins to be the principal mediators of cell adhesion. For other T-cell subtypes it was reported that mucosal T cells mainly use the $\alpha 4\beta 7$ integrin to infiltrate into gut tissues (29, 30), whereas the migration of CD8 T cells into mouse lung tissues is mediated predominately by LFA-1 (31).

In conclusion, we have demonstrated a highly sensitive method to quantify the adhesive strength of lymphocyte–endothelial interaction following various contact conditions. This technique is not limited to the chosen model system and can potentially be used to study a broad range of cell–cell or cell–substrate interactions in various disease-oriented settings. Moreover, our characterization of the Jurkat/HUVEC interaction is far from being complete. For example, it should also be noted that the relative contributions of the different adhesion molecules reported here are for conditions of 250 msec of contact and a compression force of 500 pN. The relative contributions of these adhesion molecules may be different under different conditions. It is likely that E-selectin plays a more prominent role than the integrin receptors at short contact duration, whereas activation of the T cells may increase the contribution of the integrin-mediated adhesion.

1. Janeway CAJ, Travers P. Immunobiology: The Immune System in Health and Disease. Current Biology Ltd/Garland Publishing Inc, 1994.
2. Steeber DA, Tedder TF. Adhesion molecule cascades direct lymphocyte recirculation and leukocyte migration during inflammation. Immunol Res 22:299–317, 2000.
3. Springer TA. Adhesion receptors of the immune system. Nature 346: 425–434, 1990.
4. Kubes P, Kerfoot SM. Leukocyte recruitment in the microcirculation: the rolling paradigm revisited. News Physiol Sci 16:76–80, 2001.
5. Risau W. Differentiation of endothelium. FASEB J 9:926–933, 1995.
6. Butcher EC. Leukocyte-endothelial cell recognition: Three (or more) steps to specificity and diversity. Cell 67:1033–1036, 1991.
7. Springer TA. Traffic signals for lymphocyte recirculation and leukocyte emigration: the multistep paradigm. Cell 76:301–314, 1994.
8. Radeke HH, Ludwig RJ, Boehncke WH. Experimental approaches to lymphocyte migration in dermatology in vitro and in vivo. Exp Dermatol 14:641–666, 2005.
9. Bousso P. Real-time imaging of T-cell development. Curr Opin Immunol 16:400–405, 2004.
10. Halin C, Rodrigo Mora J, Sumen C, von Andrian UH. In vivo imaging of lymphocyte trafficking. Annu Rev Cell Dev Biol 21:581–603, 2005.
11. Binnig G, Quate CF, Gerber C. Atomic force microscope. Phys Rev Lett 56:930–933, 1986.
12. Hansma HG, Pietrasanta L. Atomic force microscopy and other scanning probe microscopies. Curr Opin Chem Biol 2:579–584, 1998.
13. Chen A, Moy VT. Single-molecule force measurements. Methods Cell Biol 68:301–309, 2002.
14. Hutter JL, Bechhoefer J. Calibration of atomic-force microscope tips. Rev Sci Instrum 64:1868–1873, 1993.
15. Benoit M. Cell adhesion measured by force spectroscopy on living cells. Methods Cell Biol 68:91–114, 2002.
16. Wojcikiewicz EP, Zhang X, Chen A, Moy VT. Contributions of molecular binding events and cellular compliance to the modulation of leukocyte adhesion. J Cell Sci 116:2531–2539, 2003.
17. Benoit M, Gabriel D, Gerisch G, Gaub HE. Discrete interactions in cell adhesion measured by single-molecule force spectroscopy. Nat Cell Biol 2:313–317, 2000.
18. Zhang X, Wojcikiewicz E, Moy VT. Force spectroscopy of the leukocyte function-associated antigen-1/intercellular adhesion molecule-1 interaction. Biophys J 83:2270–2279, 2002.
19. Evans E, Leung A, Hammer D, Simon S. Chemically distinct transition states govern rapid dissociation of single L-selectin bonds under force. Proc Natl Acad Sci U S A 98:3784–3789, 2001.
20. Tees DF, Waugh RE, Hammer DA. A microcantilever device to assess the effect of force on the lifetime of selectin-carbohydrate bonds. Biophys J 80:668–682, 2001.
21. Schneider U, Schwenk HU, Bornkamm G. Characterization of EBV-genome negative "null" and "T" cell lines derived from children with acute lymphoblastic leukemia and leukemic transformed non-Hodgkin lymphoma. Int J Cancer 19:621–626, 1977.
22. Osborn L, Hession C, Tizard R, Vassallo C, Luhowskyj S, Chi-Rosso G, Lobb R. Direct expression cloning of vascular cell adhesion molecule 1, a cytokine-induced endothelial protein that binds to lymphocytes. Cell 59:1203–1211, 1989.
23. Chan JR, Hyduk SJ, Cybulsky MI. Alpha 4 beta 1 integrin/VCAM-1 interaction activates alpha L beta 2 integrin-mediated adhesion to ICAM-1 in human T cells. J Immunol 164:746–753, 2000.
24. Smith CW, Rothlein R, Hughes BJ, Mariscalco MM, Rudloff HE, Schmalstieg FC, Anderson DC. Recognition of an endothelial determinant for CD 18-dependent human neutrophil adherence and transendothelial migration. J Clin Invest 82:1746–1756, 1988.
25. Florin EL, Moy VT, Gaub HE. Adhesion forces between individual ligand-receptor pairs. Science 264:415–417, 1994.
26. Zhang X, Craig SE, Kirby H, Humphries MJ, Moy VT. Molecular basis for the dynamic strength of the integrin alpha4beta1/VCAM-1 interaction. Biophys J 87:3470–3478, 2004.
27. Bell GI. Models for the specific adhesion of cells to cells. Science 200: 618–627, 1978.
28. Evans E, Heinrich V, Leung A, Kinoshita K. Nano- to microscale dynamics of P-selectin detachment from leukocyte interfaces. I. Membrane separation from the cytoskeleton. Biophys J 88:2288–2298, 2005.
29. Shigematsu T, Specian RD, Wolf RE, Grisham MB, Granger DN. MAdCAM mediates lymphocyte-endothelial cell adhesion in a murine model of chronic colitis. Am J Physiol Gastrointest Liver Physiol 281: G1309–G1315, 2001.
30. Berlin C, Bargatze RF, von Andrian UH, Szabo MC, Hasslen SR, Nelson RD, Berg EL, Erlandsen SL, Butcher EC. $\alpha 4$ integrins mediate lymphocyte attachment and rolling under physiologic flow. Cell 80: 413–422, 1995.
31. Thatte J, Dabak V, Williams MB, Braciale TJ, Ley K. LFA-1 is required for retention of effector CD8 T cells in mouse lungs. Blood 101:4916–4922, 2003.